INDONESIAN MINING JOURNAL Vol. 28, No. 1, April 2025 : 31 - 44

DISTRIBUTION AND CORRELATION OF CRITICAL MINERALS Pb-Zn SKARN DEPOSITS IN CIHAUR VILLAGE, SUKABUMI DISTRICT, WEST JAVA

SEBARAN DAN KORELASI MINERAL KRITIS PADA ENDAPAN SKARN Pb-Zn DI DESA CIHAUR, KABUPATEN SUKABUMI, JAWA BARAT

KHAIRU RIZAL[1*], NURKHAMIM[1] and ARIFUDIN IDRUS[2]
[1] Master of Mining Engineering Program, UPN "Veteran" Yogyakarta,
Jl. Padjajaran, Sleman, Yogyakarta, Indonesia.
[2] Department of Geological Engineering, Faculty of Engineering, Gadjah Mada University,
Jl. Grafika Bulaksumur No.2, Senolowo, Sinduadi, Kec. Mlati, Sleman Regency, Yogyakarta
* Author's corresponding e-mail: rizalmarsyaf@gmail.com

ABSTRACT

This research investigates ore samples from Cihaur Village, Sukabumi District, West Java, which exhibit significant skarn alteration in limestone, is examined for its petrographic and mineragraphic features. Secondary minerals identified include pyroxene, garnet, calcite, and opaque minerals, while the primary ore minerals are chalcopyrite ($CuFeS_2$), galena (PbS), and sphalerite (ZnS). Five samples were analyzed geochemical analysis using the ICP-MS method to assess the concentration of important elements including Pb, Zn, Cu, Ag, Sb, Bi, Cd, Mg, Al, Ca, Fe, and As. Element distribution patterns were examined using spider diagrams, providing insight into environmental gradients influencing mineral exploration. The study revealed a high positive correlation between Pb and Zn, suggesting co-deposition in sulfide mineralization. Pb also correlates strongly with Ag and Sb. This study confirms the considerable economic potential of the Sukabumi skarn deposits for Pb, Zn, Cu, and precious metals such as Ag. Exploration value is increased when essential minerals like Sb and Cd are present. Variations in geochemical conditions indicate the influence of magmatic intrusions and hydrothermal activity on element distribution. These results provide a solid foundation for further exploration to delineate mineralization zones in the region.

Keywords: critical minerals, mining, geochemical, distribution, correlation.

ABSTRAK

Penelitian ini mengkaji sampel bijih dari Desa Cihaur, Kabupaten Sukabumi, Jawa Barat yang menunjukkan perubahan skarn yang signifikan pada batugamping. Sampel ini dianalisis berdasarkan karakteristik petrografi dan mineragrafi. Mineral sekunder yang teridentifikasi meliputi piroksen, garnet, kalsit, dan mineral opak, sedangkan mineral bijih primernya adalah kalkopirit ($CuFeS_2$), galena (PbS), dan sfalerit (ZnS). Lima sampel dianalisis secara geokimia menggunakan metode ICP-MS untuk mengetahui keberadaan unsur-unsur mineral kritis termasuk Pb, Zn, Cu, Ag, Sb, Bi, Cd, Mg, Al, Ca, Fe, dan As. Pola distribusi unsur-unsur tersebut dianalisis menggunakan diagram spider, yang menjelaskan gradien lingkungan yang mempengaruhi eksplorasi mineral. Hasil penelitian menunjukkan adanya korelasi positif yang kuat antara, Pb dan Zn, yang mengindikasikan adanya pengendapan bersama dalam mineralisasi sulfida. Selain itu, Pb juga memiliki korelasi yang kuat dengan Ag dan Sb. Studi ini menegaskan potensi ekonomi yang besar dari endapan skarn di Sukabumi untuk unsur Pb, Zn, Cu, dan logam mulia seperti Ag. Nilai prospek eksplorasi juga meningkat dengan adanya mineral esensial seperti Sb, dan Cd. Variasi kondisi geokimia mengindikasikan pengaruh intrusi magma dan aktivitas hidrotermal terhadap distribusi elemen yang terlihat di berbagai lokasi. Hasil ini memberikan landasan yang kuat untuk eksplorasi lanjutan serta rekomendasi penelitian tambahan yang bertujuan mengidentifikasi zona mineralisasi paling prospektif di wilayah tersebut.

Kata kunci: mineral kritis, tambang, geokimia, distribusi, korelasi.

Received: 12-02-2025, first revision: 06-03-2025, second revision: 10-03-2024, accepted: 24-03-2025.
DOI: 10.30556/imj.Vol28.No1.2025.1655

INTRODUCTION

Countries around the world are increasingly recognizing the importance of securing critical mineral supplies to support their strategic and technological industries (Nassar *et al.*, 2020). These critical minerals are vital for a wide range of high-tech applications, including computers, mobile phones, televisions, laser beams, missile weapons and electric vehicles. In the era of advanced technology, rare earth elements (REEs) are particularly valued as environmentally friendly and strategically important raw materials for future energy system, especially given the growing demand for clean energy and the associated risks to supply security (Tampubolon *et al.*, 2024).

The findings of studies on Pb-Zn skarn mineralization in Ruwai, Lamandau Regency, Central Kalimantan, conducted by Idrus and Wardhani (2011), Idrus, Setijadji and Thamba (2011), Budiawan, Bargawa and Idrus (2022), Dana *et al.* (2022), and Idrus *et al.* (2023), indicate that the ore minerals are primarily composed of galena (PbS), sphalerite (ZnS), chalcopyrite ($CuFeS_2$), and pyrite (FeS_2). Geochemical analysis reveals high concentrations of base metals such as Pb, Zn, Cu, and with Zn showing the higher concentration among them, reaching up to 50,000 ppm. Whole rock geochemical studies also show enrichment in Ag, Nb, Co, La, Cu, V, Zr, Ti, and As. Pb, and Se. The silver concentration, which reaches 0.45 weight percent, is most likely transported by the mineral galena (argentiferous galena).

This study aims to determine the distribution and correlation of critical minerals in the Pb-Zn skarn deposits of Sukabumi, West Java. The Sukabumi area was selected due to its distinctive geochemical characteristics and significant economic potential. Geologically, the region lies within the Sunda-Banda magmatic arc, which dates back to the Miocene Epoch. The interaction between the Ciemas dacite intrusions and the limestones of the Jampang Formation led to the development of an exoskarn-type Pb-Zn skarn system, characterized by well-defined mineralogical zonation.

GEOLOGY

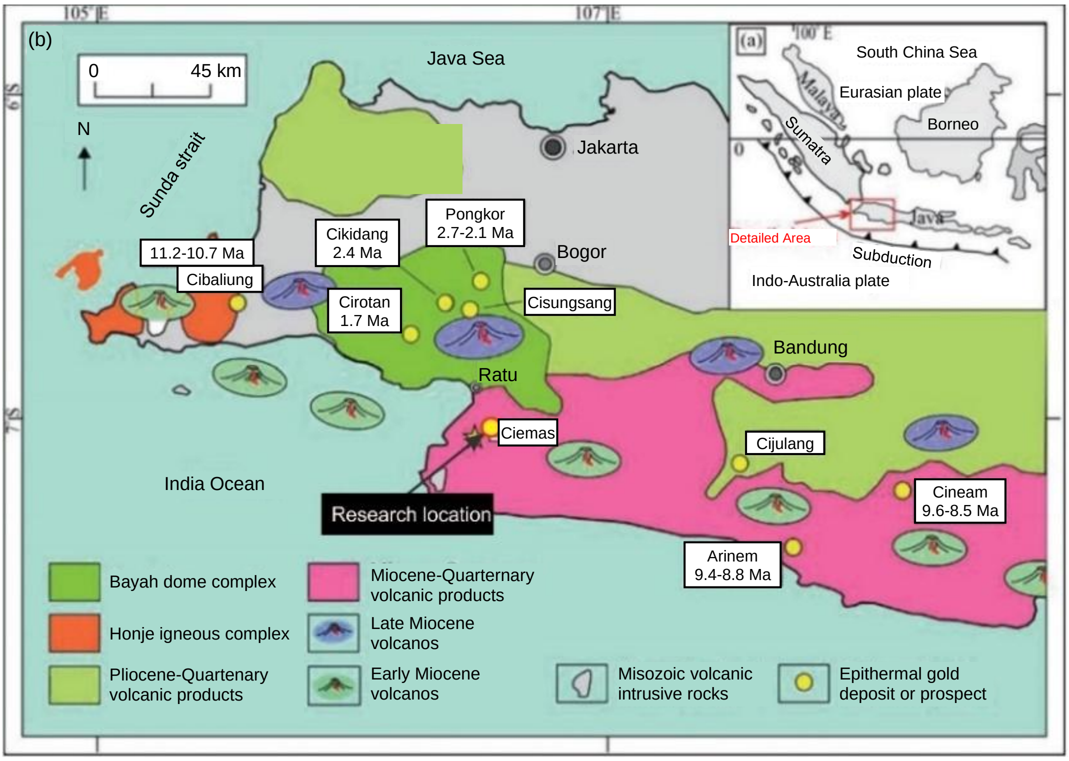

sources: (Zheng *et al.*, 2017)

Figure 1. Map of West Java regional magmatism from (Zheng et al., 2017)

West Java is located in the western segment of the Sunda continental convergent arc, part of the central Banda region. This arc contains two belts of Cenozoic magmatism (Zheng *et al.*, 2017) (Figure 1). Regionally, the Simpenan site lies within a complex of Miocene and Quaternary are separated by the Pliocene volcanic rocks located in the southeastern part of the Bayah Dome complex. Mineralization in this complex is associated with Miocene (~17 Ma) magmatism (Wu *et al.*, 2015). The geological map of the Jampang and Balekambang Sheets depicts the geology of the Cihaur- Simpenan area is underlain by a single formation, the Early Miocene Jampang Formation. The Lower Jampang Formation consists of carbonate tuff breccia composed of dacite, and andesite, globigerina marl, sandstone and thick layers of foraminifera limestone. The Upper Jampang Formation consists of volcanic tuff breccias with limestone lenses and nodules, dikes, sills, andesitic and dacitic stocks, and quartz veins (Zhang *et al.*, 2015).

The local geology (Figure 2) indicates that the study area is underlain by lapilli tuff, andesite, and dacite. Identified hydrothermal alteration types include silicic (quartz), silica-clay (quartz-kaolinite), propylitic (chlorite), and argillic (smectite-kaolinite). Three ore mineralization assemblages have been recognized pyrrhotite-chalcopyrite, massive pyrite, and galena-sphalerite. Skarn alteration in the area progresses from prograde to retrograde stages. Clinopyroxene and wollastonite are typical of the prograde stage, while the retrograde stage is marked by the presence of chlorite, epidote and calcite (Arsah *et al.*, 2023).

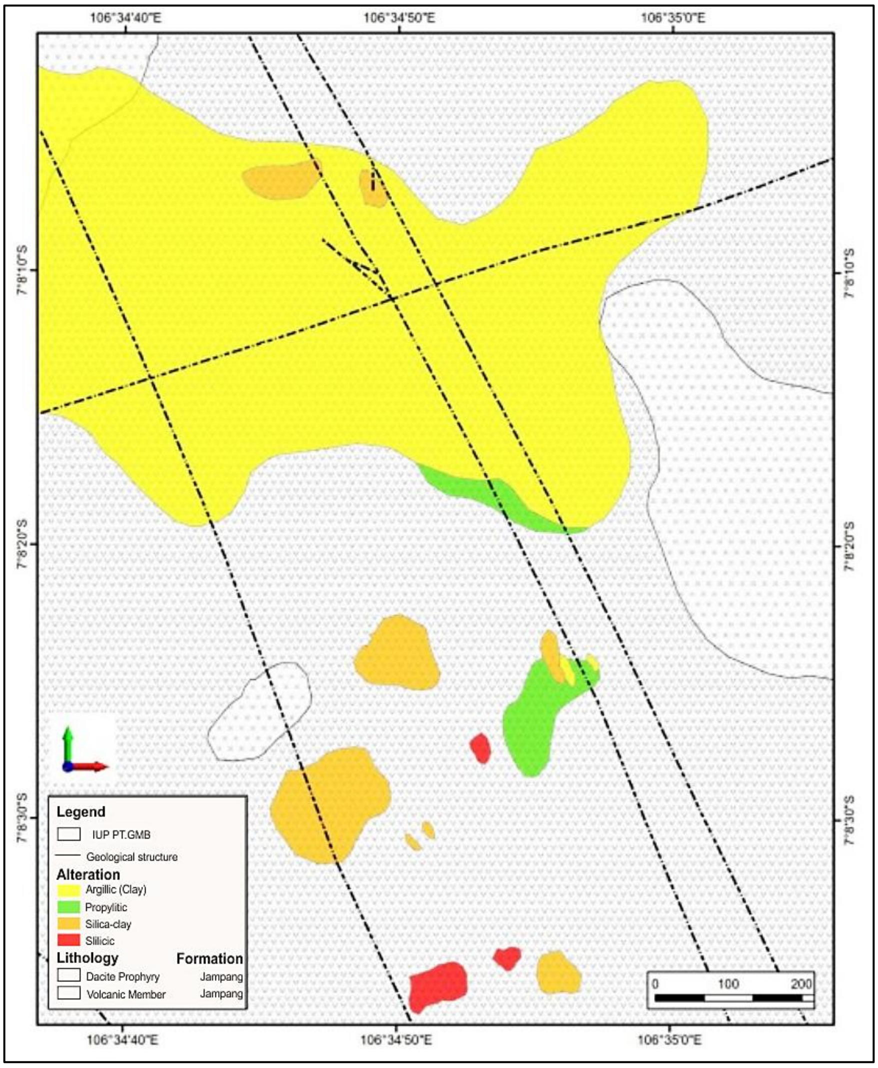

Figure 2. Geological map of the study area (PT. Generasi Muda Bersatu)

METHODOLOGY

In this study, five drill core samples were collected from drill sites ZK-A, ZK-C, ZK-B, ZK-D, and ZK-E. These samples were obtained from the exploration activities of PT Generasi Muda Bersatu (GMB) in Cihaur, Sukabumi, West Java (Table 1 and Figure 3). Three laboratory methods were applied in this study, including petrography, ore microscopy, and Inductively Coupled Plasma-Mass Spectrometry (ICP-MS). From the five boreholes, three polished sections of ore and three thin sections of skarn were prepared for analysis (Figure 3). Petrographic and ore microscopy analyses were conducted at Geomineral Sukma Analysis, Gondokusuman, Yogyakarta, using a Bestscope 5062TTR polarizing microscope. The primary objective of these analyses was to identify and characterize the minerals and ores within the skarn deposit. To assess mineral abundance, the study applied Kingston Morrison Limited (1997) visual estimation method, with categorizes proportions based on visual abundance.

Table 1. Sample coordinate data

Sample Code	X	Y	Deepth
ZK-A	674734.042	9210741.485	93.80–94.00
ZK-B	674804.360	9210978.900	71.80-72.00
ZK-C	674714.863	9210638.102	85.80-85.95
ZK-D	674672.192	9210713.734	106.95-107.90
ZK-E	675007.200	9210987.000	76.00-77.10

Inductively Coupled Plasma-Mass Spectrometry (ICP-MS) was used to analyze the concentrations of Pb, Zn, Cu, Ag, Sb, Bi, Cd, Mg, Al, Ca, Fe, and As in all samples from the study area. The analysis was conducted at the Indo Mineral Research Laboratory, Purwakarta District, Indonesia. The ICP-MS procedure involved acid digestion in Teflon tubes. Prior to analysis, the samples were dried, crushed using a jaw crusher or iron hammer and pulverized with a mill. The rock sample solution for ICP-MS analysis was prepared by acid digestion of fused glass grains. The resulting elemental concentrations were further evaluated using linear regression and Pearson correlation to determine relationship between the various elements.

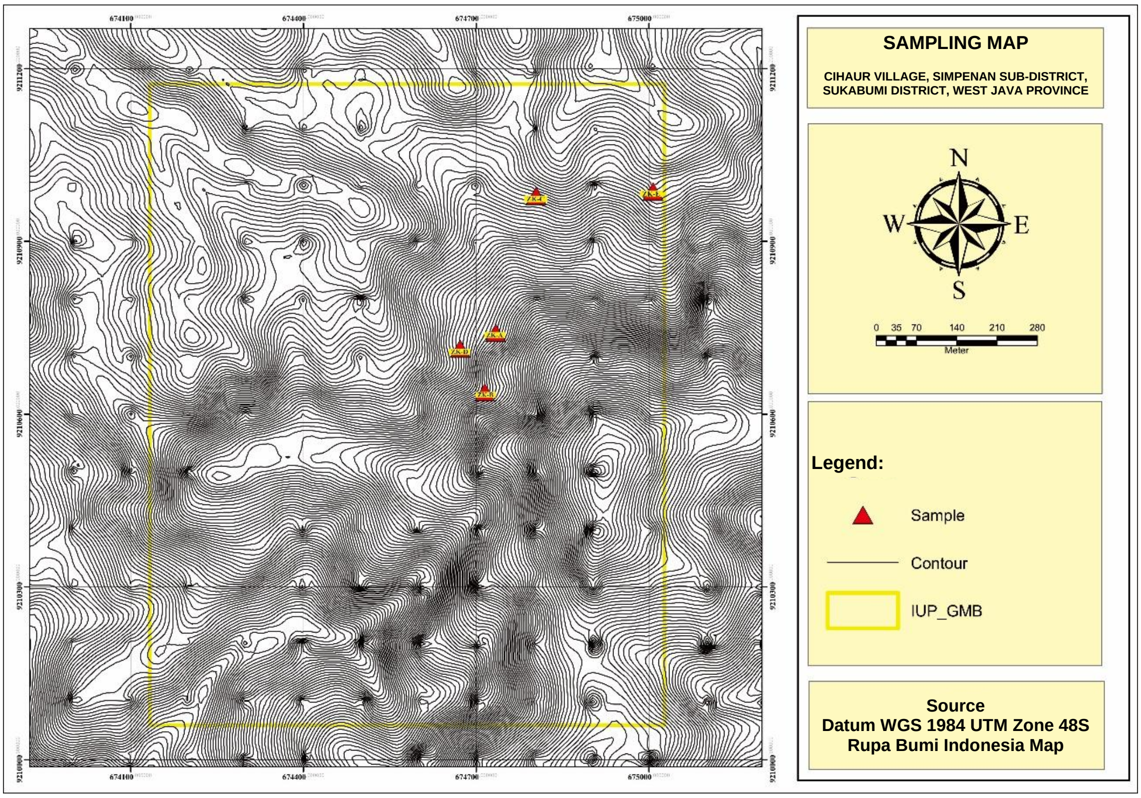

Figure 3. Sampling map of the study area

RESULTS

Petrography and Mineragraphy

At The Cihaur Village, Sukabumi District, West Java, megascopic observations (Figure 4A, B, C) indicate that the rock is a limestone that has undergone intense skarn alteration. It displays a greenish yellow color with a massive and compact texture and contains secondary mineral such as pyroxene, garnet, calcite, opaque minerals (Figure 4D, E, F). Microscopic analysis of thin and polished sections reveals textures and mineral assemblages characteristic of skarn deposits. Pyroxene (Px), comprising approximately 10% of the sample, occurs as crystals ranging from 0.1 to 1.5 mm in size. The crystals are typically subhedral to anhedral, exhibiting oblique extinction angles and second-order yellow to brown interference colors under crossed nicols. Garnet (Grt) is present in minor amounts (<1%) with crystal size ranging from 0.5 to 2 mm and typically display euhedral to subhedral shape. Under reflected light (cross nicols), garnet exhibits a characteristic zoned texture, high relief, and first order black interference colors, without an extinguishing angle. Calcite (Cal) is relatively abundant, comprising approximately 20% of the sample. It has medium to low relief, very fine crystal size, and displays third-order green-pink (pastel) interference colors under cross nicols. Calcite also shows parallel darkening but lacks noticeable cleavage or a dominant crystal habit. Opaque mineral (Op) dominate the samples, making up about 80% of the mineral composition. These minerals appear black in color, with subhedral to anhedral shapes, fine crystal sizes, and medium relief under cross nicols. As shown in Figures 4G, 4H dan 4I, the primary ore minerals identified through polished section analysis include galena, sphalerite, pyrite, and chalcopyrite. The textural relationships among these ore minerals indicate a multi-stage mineralization process within a skarn setting.

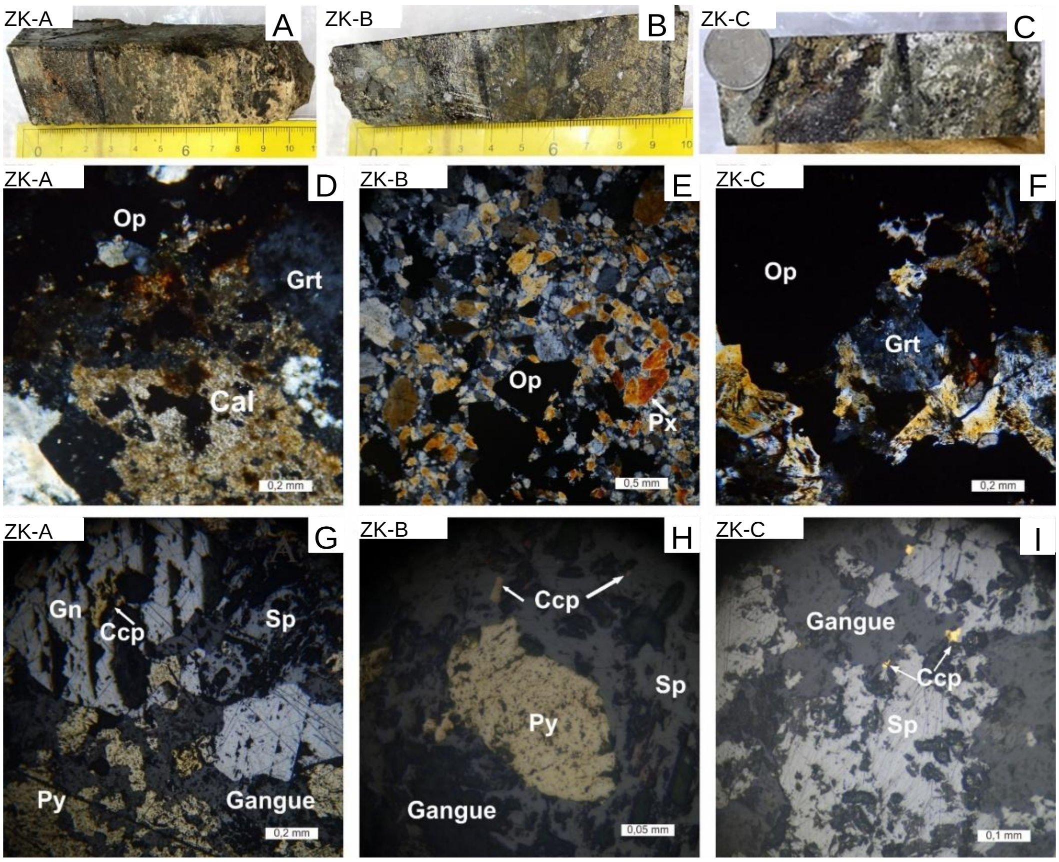

Figure 4. (A-C) megascopic photograph of samples, (D-F) photomicrograph of skarn mineral assemblages, showing mineral pyroxene (Px), garnet (Grt), calcite (Cal) and opaque mineral (Op) (cross nicols), (G-I) ore microscopy microphotos showing minerals galena (Gn), sphalerite (Sp), chalcopyrite (Ccp), and pyrite (Py) (under cross nicols).

Microscopic examination under reflected light (cross nicols) reveals a polymetallic sulfide assemblage dominated by galena (Gn), which constitutes approximately 50% of the mineral content. This is followed by sphalerite (Sp) at 20%, pyrite (Py) at 15%, and subordinate chalcopyrite (Ccp) at 5% (Figures 2D and 2E). Galena (PbS) exhibits white reflectance and strong anisotropism. It occurs as subhedral to anhedral grains ranging from 0.05 to 1.5 mm in size, characterized by two-directional cleavage planes and distinctive triangular pit textures. Neither pleochroism nor bireflectance is observed. Chalcopyrite ($CuFeS_2$) appears as pale yellow to orange subhedral to euhedral crystals (0.05–1.5 mm) with high reflectance. It occurs both as discrete grains and as "chalcopyrite disease" inclusions within sphalerite, indicating exsolution textures during cooling. Sphalerite (ZnS) exhibits moderate reflectance with gray coloration and subhedral morphology (1–4.5 mm). It displays weak one-directional cleavage and lacks both pleochroism and bireflectance. Chalcopyrite inclusions are commonly disseminated within this phase. Pyrite (FeS_2) forms cubic to subhedral-anhedral crystals (0.1–0.7 mm) with bright yellow reflectance, high relief, and prominent one-directional cleavage. It shows no pleochroism, consistent with its isotropic properties.

Geochemical Data

Five ore samples (ZK-A, ZK-C, ZK-B, ZK-D, and ZK-E) were analyzed using Inductively Coupled Plasma Mass Spectrometry (ICP-MS) to determine the content of various critical mineral elements. The analyzed elements include silver (Ag), bismuth (Bi), cadmium (Cd), antimony (Sb), zinc (Zn), lead (Pb), iron (Fe), aluminum (Al), copper (Cu), magnesium (Mg), calcium (Ca), and arsenic (As), with results reported in parts per million (ppm). The analytical data presented in Table 2 provide insight into the geochemical characteristics of the samples and indicated the potential presence of critical minerals with economic importance for mineral exploration.

Table 2. Inductively coupled plasma mass spectrometry (ICP-MS) data

Samples	ZK-A	ZK-B	ZK-C	ZK-D	ZK-E
	part per million (ppm)				
Ag	3.45	9.90	0.72	4.15	2.15
Al	9,30273	2,728.86	16,911.48	3,462.84	4,556.18
As	5.40	335.99	130.23	1.32	1.08
Ba	8.68	3.07	3.28	4.67	6.42
Be	0.87	0.04	0.56	0.01	0.02
Bi	58.18	0,25	43.51	bdl	bdl
Ca	24,577.88	1,259.12	36,546.32	3,883.23	7,192.22
Cd	331.29	422.44	456.76	0.25	0.15
Ce	4.83	0.63	2.79	0.28	0.44
Co	58.63	26.50	11.25	85.93	96.20
Cr	23.53	44.79	36.57	501.65	60.09
Cs	0.16	0.13	0.13	0.03	0.04
Cu	1,224.88	1,332.36	1,012.17	43.18	6.29
Dy	0.52	0.05	0.37	0.03	0.03
Er	0.25	0.03	0.17	0.02	0.02
Eu	0.29	0.02	0.25	0.01	0.02
Fe	357,992.53	403,169.72	206,495.72	48,803.38	55.258,25
Ga	7.19	3.38	7.53	1.24	1.62
Gd	0.29	0.03	0.17	0.01	0.02
Hf	0.52	0.42	0.64	0.27	0.33
Ho	0.12	0.01	0.09	0.01	0.01
In	6.17	1.74	17.97	bdl	bdl
K	701.10	322.82	253.32	242.05	232.30
La	2.58	0.34	1.19	0.12	0.20
Li	3.54	2.36	5.90	1.77	1.18
Lu	0.03	0.01	0.03	0.01	0.01
Mg	7,810.88	1,584.47	8,661.77	178,841.66	201,787.10
Mn	4,697.19	2,298.64	3,776.75	829.18	929.39
Mo	0.77	3.11	1.74	0.84	3.33
Na	864.57	652.73	497.27	556.23	547.89

Samples	ZK-A	ZK-B	ZK-C	ZK-D	ZK-E
	part per million (ppm)				
Nb	0.77	0.61	0.53	0.04	0.18
Nd	2.34	0.29	1.56	0.13	0.15
Ni	171.47	bdl	bdl	3,599.43	2,857,69
P	281.54	74.49	132.90	bdl	1.05
Pb	29,754.30	80,279.03	166.48	33.52	2.09
Pr	0.57	0.07	0.36	0.04	0.04
Rb	2.10	0.31	0.37	0.35	0.35
Re	bdl	bdl	0.00	bdl	bdl
Sb	3.9	60.63	1.26	0.22	0.29
Sc	3.87	0.39	7.67	7.69	9.85
Se	0.57	0.97	0.43	0.44	0.37
Sm	0.55	0.05	0.39	0.02	0.02
Sn	26.48	40.66	29.35	1.72	2.05
Sr	24.72	1.83	28.95	2.19	2.10
Ta	0.12	0.04	0.08	bdl	0.01
Tb	0.05	0.01	0.04	0.00	0.00
Te	0.70	bdl	0.05	bdl	bdl
Th	0.59	0.27	0.68	0.06	0.07
Ti	324.75	54.85	515.31	60.18	54.97
Tl	0.07	0.10	0.05	0.06	0.05
Tm	0.04	0.01	0.03	0.01	0.01
U	1.50	0.34	2.13	0.02	0.02
V	29.61	4.91	60.74	25.11	3044
W	0.82	0.54	1.52	0.35	0.24
Y	5.64	0.47	3.03	0.23	0.32
Yb	0.24	0.03	0.23	0.04	0.05
Zn	76,706.45	126,768.94	92,226.93	74.60	25.81
Zr	23.94	19.71	22.57	12.68	14.76

Note: bdl = below detection limit

Table 2 presents ICP-MS geochemical analysis data shows a geochemical profile consistent with a Pb-Zn skarn deposit characterized by substantial mineralization. The highest concentrations of Zn (25.81-126,768 ppm), Pb (2.09-32,500 ppm), and Ag (0.72-9.90 ppm), indicating a mature skarn mineralization system with well defined geochemical zonation. The high Fe content (55,258.25-206,495.72 ppm) reflects intense sulfidation during the retrograde stage, while the Cu concentrations (6.29-1,332.36 ppm) suggest magmatic fluid involvement during the early mineralization phase (Meinert, 1987). The presence of pathfinder elements as Te (0.05-0.70 ppm), Sb (0.22-3.96 ppm), Cd (0.15-456.76), In (1.74-17.97 ppm), and Bi (0.25-58.18 ppm) further highlights the deposit's additional economic potential. High fluctuations in Sb and As concentrations (1.08-335.99 ppm) suggest a hydrothermal gradient from the proximal to distal zones. The research area is likely situated within the intermediate to distal zone of the intrusion source, which is significant for defining exploration vectors. This interpretation is supported by the pathfinder elements ratio (As/Sb = 0.08-1.35), indicating a shift from proximal to distal zones (Sader and Ryan, 2020). High base metal concentrations emerge during the cooling stage of hydrothermal fluids, according to the geochemical data, supporting the hypothesis of Pb-Zn skarn formation through a prograde-retrograde process (Meinert, 1987).

The process of classification and characterization of igneous rocks are ~~is~~ essential for understanding the geological history and formation processes of a region. Some petrogenetic diagrams (Figure 5) are used for rock classification, geochemical analysis, and interpretation of their tectonic environment of origin.

The Zr/Ti versus Nb/Y plot is based on immobile elements (Pearce, 1996) (Figure 5a). The Quaternary to Miocene volcanic rock samples analyzed in this study show compositions similar to those reported in previous studies (Rosana and Matsueda, 2002; Harijoko *et al.*, 2004; Yuningsih *et al.*, 2012; Tun *et al.*, 2014; Wu *et al.*, 2015; Zhang *et al.*, 2015; Zheng *et al.*, 2017). Specifically, one sample plots in the harijokoandesite (diorite) plane, one mafic sample in the rhyolite-dacite (granite-granodiorite) plane, one sample in the trachyte (syenite) plane, and one sample in the alkaline rhyolite (granite) plane showing compositional variations from intermediate to acidic rocks with a tendency to be more alkaline. Most of the samples are calc alkaline metaluminous which is typical for igneous rocks from magmatic arc or subduction tectonic settings, although one is weakly peraluminous indicating possible alumina enrichment due to magma differentiation or interaction with continental crust (Barton and Young, 2002) (Figure 5b). The plot of Y versus La versus Nb (Figure 5d), used to determine the tectonic classification of the mafic igneous rocks, shows that two samples belonging to the transitional arc, one in alkaline arc, one in calc-alkaline arc, and one in late-to post-orogenic intra-continental arc. These result domains indicates that the rocks likely originated from subduction zones, which are commonly associated with active magmatic arcs (modified from Cabanis and Lecolle, 1989). The ternary diagram classifies carbonatite rocks based on CaO, MgO and FeO content (Figure 5c). Most of the samples fall between ferrocarbonatite and magnesiocarbonatite, suggesting either a differentiation process of the carbonatite magma or interaction with iron- and magnesium-rich mantle rocks, based on the International Union of Geological Sciences (IUGS) Carbonatite Rock Classification (Lustrino *et al.*, 2020).

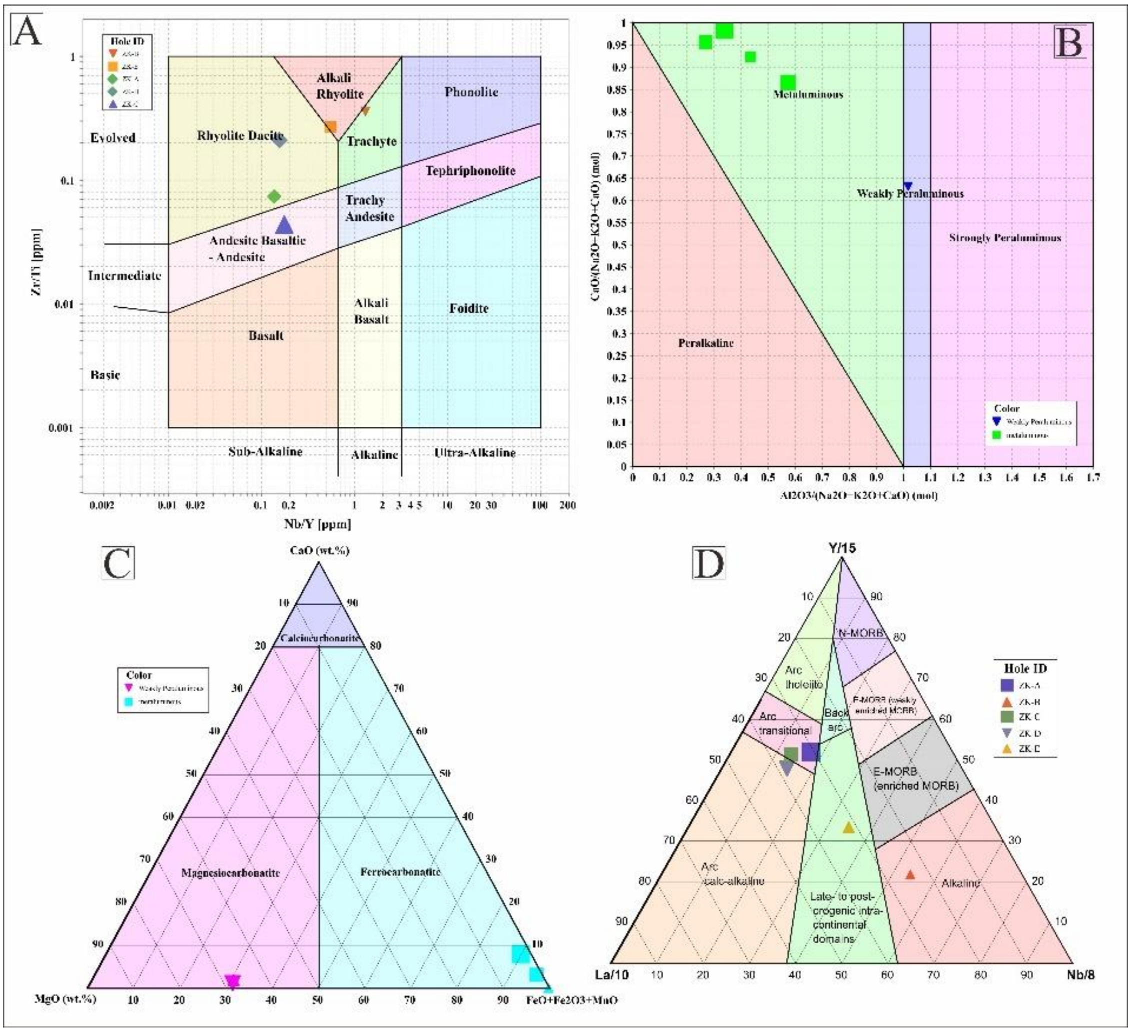

Figure 5. Bulk rock geochemical characteristics of Sukabumi intrusions, a) Nb/Y versus Zr/Ti rock classification (modified from Pearce 1996), b) Alumina Saturation Level (Barton and Young, 2002), c) International Union of Geological Sciences (IUGS) Carbonatite Rock Classification, d) Tectonic classification of Y versus La versus Nb mafic igneous rocks (modified from Cabanis and Lecolle, 1989).

Critical Mineral Distribution

In this study, the distribution patterns of rare earth elements (REEs) and critical metals (e.g., Pb, Zn, Ag, Bi, Sb) (European Commission, 2020) were analyzed using chondrite-normalized and primitive mantle-normalized spider diagrams (Figure 6) to decipher fluid evolution trends and metal enrichment mechanisms. These geochemical vectors provide critical insights into distal to proximal gradients relative to the intrusion, supporting predictive targeting of high-grade Zn-Pb-Ag zones in skarn environments (Cooke *et al.*, 2014).

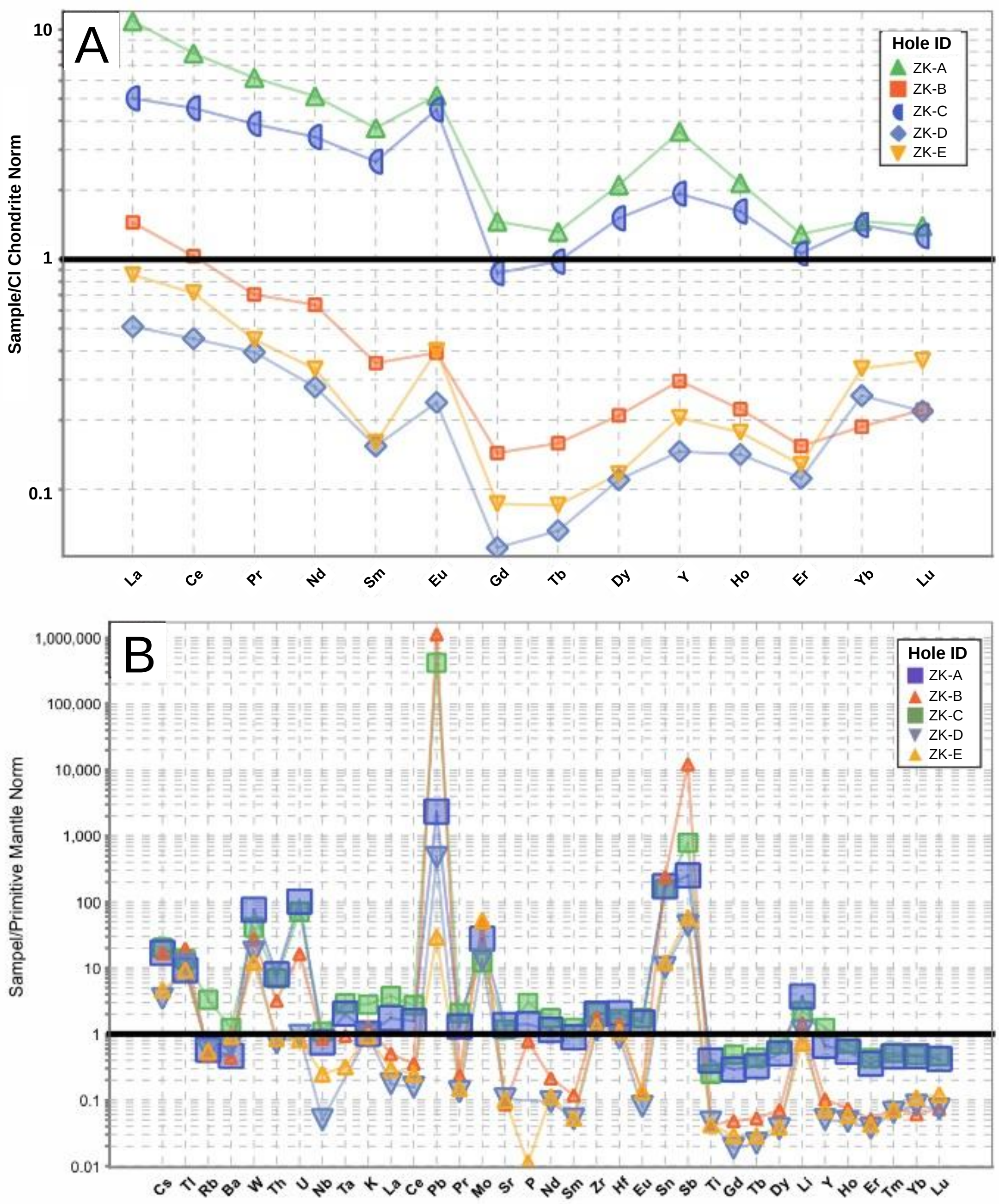

Figure 6. a) REE spider diagram normalized to CI chondrite values, using the normalization values from McDonough and Sun (1995), b) primitive mantle Norm showing W, U, Pb, Mo, Sn, and Sb rich (data is plotted on the diagram Sun and McDonough, (1989))

Certain elements show significant variations between sites (e.g., elements at the center and end of the X-axis). These anomalies may reflect the influence of localized geochemical processes, such as magma differentiation, hydrothermal activity, or the remobilization of elements by fluids. In the REE plots, all samples are characterized by a relatively similar pattern in the diagram normalized to C1 Chondrite values (McDonough and Sun, 1995) (Figure 6a). There are two distribution trend patterns that indicate some elements have higher values than the normalized line (possibly enriched elements), while others have lower values (depleted elements). These distribution patterns can help identify magma differentiation processes, hydrothermal alteration, or specific enrichment due to mineralization processes. Most samples (regardless of age or lithology) have the same LREE/HREE enrichment pattern as the negative Eu anomalies. When normalized to the primitive mantle (Sun and McDonough, 1989) (Figure 6b), most samples are enriched with relatively similar large-ion lithophile elements (LILE, e.g. U) and LREE (e.g. La, Ce, Pr, Nd) and have varying degrees of depletion of HFSE (e.g. Eu and Gd) and HREE.

The presence of Ag indicates high reducing conditions during early stages of mineralization (Idrus, Setijadji and Thamba, 2011; Dana *et al.*, 2022). Bismuth (Bi) shows significant anomalies in several samples, especially in area where Pb and Ag concentration are high. Elements such as Sb, As, and other critical minerals appear more prominently, reflecting changes in fluid chemistry as it migrates away from the heat source.

Pb, Zn, and significant minerals correlation to determine the association

The correlation between Pb, Zn and critical mineral elements was determined using a bivariate statistical approach, specifically by calculating Pearson correlation coefficients. The analysis of bivariate statistics using the Microsoft Excel program resulted in a pearson correlation coefficient.

As shown in Table 3, the yellow color highligts the magnitude of correlation value. Correlation coefficients between 0.5 and 0.7 (or -0.5 and -0.7) indicate a moderate positive (or negative) correlation, while values above 0.7 (or below -0.7) indicate a strong positive (or negative) correlation.

Based on these results, Zn, Cu, Cd, Fe, and Mg are closely related in the ore samples, which suggests that they could have comparable mineral hosts or geochemical behaviors. This is most likely due to co-precipitation during the production of skarn. Strong correlations between Pb, Ag, Sb, and Fe suggest a paragenetic connection that may be related to the mineralization of galena or sulfosalt. Whereas the high negative connection between As and Al could suggest different mineralogical controls or alteration processes, the negative correlation between Mg and Ca might represent mineralogical partitioning between carbonate and silicate phases.

Table 3. Pearson correlation calculation results of Pb, Zn, Cu, Ag, Sb, Bi, Cd, Mg, Al, Ca, Fe, and As in Pb-Zn skarn ore samples. Highlighted yellow color indicates moderately positive or negative (*) to strong (**) correlation values.

r	Pb	Zn	Cu	Ag	Sb	Bi	Cd	Fe	As	Mg	Al	Ca
Pb	1,00											
Zn	0,75**	1,00										
Cu	0,70*	0,96**	1,00									
Ag	0,91**	0,48	0,39	1,00								
Sb	0,95**	0,69*	0,57*	0,93**	1,00							
Bi	-0,12	0,38	0,57*	-0,46	-0,35	1,00						
Cd	0,54*	0,96**	0,95**	0,23	0,48	0,57*	1,00					
Fe	0,84**	0,91**	0,96**	0,57*	0,68*	0,43	0,83**	1,00				
As	0,82**	0,81**	0,64*	0,74**	0,92**	-0,22	0,67*	0,65*	1,00			
Mg	-0,59*	-0,95**	-0,99**	-0,28	-0,47	-0,64*	-0,98**	-0,90**	-0,60*	1,00		
Al	-0,38	0,32	0,36	-0,66*	-0,42	0,78**	0,56*	0,11	-0,09	-0,50	1,00	
Ca	-0,37	0,31	0,40	-0,67*	-0,47	0,88**	0,55*	0,17	-0,18	-0,52*	0,98**	1,00

DISCUSSION

Statistical analysis was conducted on the Pb, Zn, and critical minerals data from Pb-Zn skarn ore samples. A strong positive correlation was observed between Pb and Zn, likely reflecting their concurrent precipitation in sulfide mineralization, such as galena (PbS) and sphalerite (ZnS), which commonly occur together in Pb-Zn skarn systems. The significant positive correlation between Pb and Zn reflects the association between galena and sphalerite at the retrograde stage of the skarn, which is common in skarn systems influenced by metal-rich hydrothermal fluids.

Ag and Sb show strong correlations with Pb, suggesting an association with galena (PbS) or argentite (Ag_2S) minerals. Elements Cd, and Zn show inclusion of Cd in sphalerite (ZnS) as ionic substituents, while Fe associates with Pb, and Zn, supporting the presence of sulfide minerals such as pyrite (FeS_2) alongside major metals. In the context of its formation, the negative correlation between metals (Pb, Zn, Cu), and Mg indicates the destruction of carbonate minerals (dolomite/magnesite) during the skarnification process. This mineral system likely evolved from high temperature (prograde) to lower temperature (retrograde) conditions, resulting in economic metal mineralization (Shu *et al.*, 2017; Ma *et al.*, 2025).

Skarn deposits in Sukabumi, particularly in the Cihaur area, have significant economic potential for base metals such as Pb, Zn, and Cu, as well as precious metals like Ag as a by-product (Badan Geologi, 2022; Direktorat Jenderal Mineral Dan Batubara, 2025). The presence of Sb, and Cd adds exploration value as strategic critical minerals. The mineralized zones in Sukabumi reflect a metamorphic contact-type skarn environment with the influence of magma fluids that increase metal concentrations. Hydrothermal fluids derived from dacite intrusions play an crucial role in transporting heavy metals to mineralized zones. The presence of carbonate rocks as the primary host rock allows metasomatic reactions to produce skarn minerals. Cracks and fault zones serve as pathways for hydrothermal fluids, allowing metal deposition along veins or permeable zones. Temperature variations during the prograde and retrograde stages determine the type of minerals formed.

The distribution of analytical grades shown in the spider diagrams reveals notable Pb and Zn anomalies, which reflect the zoning pattern typical of mineralization skarn-hydrothermal systems. Sites with high Pb levels (such as at ZK-B and ZK-A) indicate potential massive sulfide mineralization zones, while sites with lower Pb levels (such as at ZK-E, ZK-D and ZK-C) indicate potential less massive sulfide mineralization zones. This is related to the geochemical conditions of the hydrothermal fluids (changes in pH, Eh, and temperature) of the Pb-Zn skarn. High Zn levels may support exploration of distal zones. Elemental concentrations fluctuations in each borehole indicate vertical distribution of mineralization following the path of the hydrothermal fluid. Concentration peaks reflect the main deposition zones. Significant differences between boreholes, especially between ZK-B, and ZK-E, compared to ZK-C, indicate significant lateral variations, influenced by changes in geochemical conditions and geological structure.

CONCLUSION AND SUGGESTION

Petrographic and mineragraphic analyses of a sample collected from Sukabumi, West Java, shows interesting petrographic and mineragraphic characteristics. Megascopically, this sample is identified as strongly skarn-altered limestone, exhibiting a greenish-yellow color and massive texture. Secondary minerals observed include pyroxene, garnet, calcite, and various opaque minerals in differing proportions. Mineralogical analysis indicated that galena (PbS) is the dominant and as the main ore mineral, accompanied by sphalerite (ZnS) and chalcopyrite ($CuFe_2$) and pyrite (FeS_2). Geochemical analysis using the ICP-MS method on five samples reveal variations in the concentration of critical elements such as Pb, Zn, Cu, Ag, Sb, Bi, Cd, Mg, Al, Ca, Fe, and As. Spider diagrams were utilized to interpret the distribution patterns of these elements, offering insights into environmental gradients and guiding mineral exploration recommendations. Several sites display complex geochemical characteristics, likely influenced by hydrothermal activity or magmatic intrusion. Notably, Pb and Zn show a strong positive correlation with Ag and Sb, whereas no significant correlation is observed between Pb and Zn with other critical minerals. This study confirms that skarn deposits in Sukabumi possess high economic potential for these metals and highlights the importance of geochemical in guiding mineral exploration efforts.

ACKNOWLEDGEMENT

This work financially supported by the Institute for Research and Community Service UPN "Veteran" Yogyakarta, in 2025. The authors would also like to express their gratitude to the Master's Program in Mining Engineering at UPN "Veteran" Yogyakarta.

REFERENCES

Arsah, I.F., Idrus, A., Handini, E., Ilmawan, I., Faruqi, M.D. and Sukadana, I.G. (2023) 'Geology and mineralogy of the Cihaur Pb-Zn skarn in Sukabumi Regency, West Java, Indonesia: A preliminary study', in H. Iswandi, T. Igarashi, C. Tabelin, T. Pasang, O.F. Ugurly, Y. Rizkianto, and O.W. Lusantono (eds) *4th International Conference on Earth Science, Mineral and Energy*. Sleman: AIP Conference Proceedings, p. 060005. Available at: https://doi.org/10.1063/5.0126047.

Badan Geologi (2022) 'Potensi dan ketahanan cadangan mineral kritis dan strategis (nikel, tembaga, emas dan perak timah, Bauksit)'. Bandung: Badan Geologi.

Barton, M.D. and Young, S. (2002) 'Non-pegmatitic deposits of beryllium: Mineralogy, geology, phase equilibria and origin', *Reviews in Mineralogy and Geochemistry*, 50(1), pp. 591–691. Available at: https://doi.org/10.2138/rmg.2002.50.14.

Budiawan, S.R.H., Bargawa, W.S. and Idrus, A. (2022) 'Karakteristik mineralisasi dan geokimia skarn Pb-Zn-Cu-Ag, Ruwai, Kabupaten Lamandau Provinsi Kalimantan Tengah', *Jurnal Sumberdaya Bumi Berkelanjutan (SEMITAN)*, 1(1), pp. 136–143. Available at: https://doi.org/10.31284/j.semitan.2022.3238.

Cabanis, B. and Lecolle, M. (1989) 'Le diagramme La/10–Y/15–Nb/8: un outil pour la discrimination des series volcaniques et la mise en evidence des processus de melange et/ou de contamination crustale', in *Comptes Rendus de l'Academie Des Sciences*. Paris: Gauthier-Villars.

Cooke, D.R., Hollings, P., Wilkinson, J.J. and Tosdal, R.M. (2014) 'Geochemistry of porphyry deposits', in *Treatise on Geochemistry*. Elsevier, pp. 357–381. Available at: https://doi.org/10.1016/B978-0-08-095975-7.01116-5.

Dana, C.D.P., Agangi, A., Takahashi, R., Idrus, A., Lai, C. and Nainggolan, N.A. (2022) 'Element mobility during formation of the Ruwai Zn-Pb-Ag skarn deposit, Central Borneo, Indonesia', *Resource Geology*, 72(1), p. e12290. Available at: https://doi.org/10.1111/rge.12290.

Direktorat Jenderal Mineral Dan Batubara (2025) *Harga minerla dan batubara acuan*, *https://www.minerba.esdm.go.id*. Available at: https://www.minerba.esdm.go.id/harga_acuan (Accessed: 24 March 2025).

European Commission (2020) *EUROP 2020: A European strategy for smart, sustainable and inclusive growth*. Brussels.

Harijoko, A., Sanematsu, K., Duncan, R.A., Prihatmoko, S. and Watanabe, K. (2004) 'Timing of the mineralization and volcanism at Cibaliung gold deposit, Western Java, Indonesia', *Resource Geology*, 54(2), pp. 187–195. Available at: https://doi.org/10.1111/j.1751-3928.2004.tb00199.x.

Idrus, A., Dana, C.D.P., Lai, C.-K., Agangi, A., Takahashi, R. and Rajagukguk, E.H. (2023) 'Proximal to distal geochemical variations of the Ruwai polymetallic skarn deposit, Central Borneo, Indonesia: Insights from sulfides chemistry and implications to exploration', *Journal of Geochemical Exploration*, 246, p. 107161. Available at: https://doi.org/10.1016/j.gexplo.2023.107161.

Idrus, A., Setijadji, L.D. and Thamba, F. (2011) 'Geology and characteristics of Pb-Zn-Cu-Ag skarn deposit at Ruwai, Lamandau Regency, Central Kalimantan', *Indonesian Journal on Geoscience*, 6(4), pp. 191–201. Available at: https://doi.org/10.17014/ijog.6.4.191-201.

Idrus, A. and Wardhani, R. (2011) 'Mineralogi dan kimia mineral alterasi prograde dan retrograde endapan skarn Pb-Zn-Cu-(Ag) Ruwai, Kabupaten Lamandau, Provinsi Kalimantan Tengah, Indonesia'.

Kingston Morrison Limited (1997) *Important hydrothermal Minerals and their significance*. 7th edn. New Zealand: Kingston Morrison Limited.

Lustrino, M., Bonin, B., Doroshkevich, A., Guo, Z., Kerr, A., Heilborn, M., Irving, T., Ivanov, A., Mitchell, R., Nakagawa, M., Natland, J.H., Pearce, J.A., Smith, B.S., Srivastava, R.K., Tappe, S., Wilson, M. and Zellmer, G. (2020) *IUGS task group on igneous rocks TGIR*, *www.iugs.org*. Available at: https://www.iugs.org/_files/ugd/f1fc07_b990fcac97df459cb2725a8983caa6f1.pdf?index=true (Accessed: 24 March 2025).

Ma, W., Liu, Y., Hou, Z., Yang, Z., Huizenga, J.M., Li, H., Yue, L., Li, Z. and Zhao, S. (2025) 'Evolution of ore fluids in the magmatic-hydrothermal Pb-Zn metallogenic system: A case study from Narusongduo deposit in the Himalayan-Tibetan orogen', *Geological Society of America Bulletin*, 137(5–6), pp. 2427–2454. Available at: https://doi.org/10.1130/B37866.1.

McDonough, W.F. and Sun, S. -s. (1995) 'The composition of the earth', *Chemical Geology*, 120(3–4), pp. 223–253. Available at: https://doi.org/10.1016/0009-2541(94)00140-4.

Meinert, L.D. (1987) 'Skarn zonation and fluid evolution in the Groundhog Mine, Central mining district, New Mexico', *Economic Geology*, 82(3), pp. 523–545. Available at: https://doi.org/10.2113/gsecongeo.82.3.523.

Nassar, N.T., Brainard, J., Gulley, A., Manley, R., Matos, G., Lederer, G., Bird, L.R., Pineault, D., Alonso, E., Gambogi, J. and Fortier, S.M. (2020) 'Evaluating the mineral commodity supply risk of the U.S. manufacturing sector', *Science Advances*, 6(8), p. eaay8647. Available at: https://doi.org/10.1126/sciadv.aay8647.

Pearce, J.A. (1996) 'A user's guide to basalt discrimination diagrams', in D.A. Wyman (ed.) *Trace Element Geochemistry of Volcanic Rocks: Application for Massive Sulphide Exploration*. Mineralogical Association of Canada, pp. 79–113.

Rosana, M.F. and Matsueda, H. (2002) 'Cikidang hydrothermal gold deposit in Western Java, Indonesia', *Resource Geology*, 52(4), pp. 341–352. Available at: https://doi.org/10.1111/j.1751-3928.2002.tb00144.x.

Sader, J.A. and Ryan, S. (2020) 'Advances in ICP-MS technology and the application of multi-element geochemistry to exploration', *Geochemistry: Exploration, Environment, Analysis*, 20(2), pp. 167–175. Available at: https://doi.org/10.1144/geochem2019-049.

Shu, Q., Chang, Z., Hammerli, J., Lai, Y. and Huizenga, J.-M. (2017) 'Composition and evolution of fluids forming the Baiyinnuo'er Zn-Pb skarn deposit, Northeastern China: Insights from laser ablation ICP-MS study of fluid inclusions', *Economic Geology*, 112(6), pp. 1441–1460. Available at: https://doi.org/10.5382/econgeo.2017.4516.

Sun, S. -s. and McDonough, W.F. (1989) 'Chemical and isotopic systematics of oceanic basalts: Implications for mantle composition and processes', *Geological Society, London, Special Publications*, 42(1), pp. 313–345. Available at: https://doi.org/10.1144/GSL.SP.1989.042.01.19.

Tampubolon, A., Syafri, I., Rosana, M.F. and Yuningsih, E.T. (2024) 'The correlation between Rare Earth Elements and tin in granite, quartz vein, and weathered granite samples, in South Bangka, Bangka Belitung Islands, Indonesia', *Bulletin of the Geological Society of Malaysia*, 77(1), pp. 73–85. Available at: https://doi.org/10.7186/bgsm77202408.

Tun, M.M., Warmada, I.W., Idrus, A., Harijoko, A., Verdiansyah, O. and Watanabe, K. (2014) 'Fluid inclusion studies of the Cijulang High-sulfidation epithermal prospect, West Java, Indonesia', in *2014 3rd International Conference on Geological and Environmental Sciences*. Singapore: ICGES, pp. 55–59.

Wu, C.-Q., Zhang, Z.-W., Zheng, C.-F. and Yao, J.-H. (2015) 'Mid-Miocene (~17 Ma) quartz diorite porphyry in Ciemas, West Java, Indonesia, and its geological significance', *International Geology Review*, 57(9–10), pp. 1294–1304. Available at: https://doi.org/10.1080/00206814.2014.908748.

Yuningsih, E.T., Matsueda, H., Setyaraharja, E.P. and Rosana, M.F. (2012) 'The Arinem Te-bearing gold-silver-base metal deposit, West Java, Indonesia', *Resource Geology*, 62(2), pp. 140–158. Available at: https://doi.org/10.1111/j.1751-3928.2012.00185.x.

Zhang, Z., Wu, C., Yang, X., Zheng, C. and Yao, J. (2015) 'The trinity pattern of Au deposits with porphyry, quartz–sulfide vein and structurally-controlled alteration rocks in Ciemas, West Java, Indonesia', *Ore Geology Reviews*, 64, pp. 152–171. Available at: https://doi.org/10.1016/j.oregeorev.2014.07.003.

Zheng, C., Zhang, Z., Wu, C. and Yao, J. (2017) 'Genesis of the Ciemas gold deposit and relationship with epithermal deposits in West Java, Indonesia: Constraints from fluid inclusions and stable isotopes', *Acta Geologica Sinica - English Edition*, 91(3), pp. 1025–1040. Available at: https://doi.org/10.1111/1755-6724.13322.